Ganterite, the barium mica $Ba_{0.5}K_{0.5}Al_2(Al_{1.5}Si_{2.5})O_{10}(OH)_2$, from Oreana, Nevada

CHI MA* AND GEORGE R. ROSSMAN

Division of Geological and Planetary Sciences, California Institute of Technology, Pasadena, California 91125-2500, U.S.A.

ABSTRACT

The barium dioctahedral layer silicate, ganterite, was identified from the Lincoln Hill dumortierite deposit near Oreana, Nevada, based on electron microprobe, electron-backscatter diffraction (EBSD), and Raman spectrum microanalyses. This phase occurs with dumortierite, barite, and muscovite in a vein specimen formed by hydrothermal alteration. Back-scattered electron images of the muscovite from this locality show extensive zonation of the BaO content with regions of high Ba concentrations up to 15 µm in dimension. Electron microprobe analyses of these regions reveal a composition $(Ba_{0.53}K_{0.37}Na_{0.05})_{\Sigma=0.95}(Al_{2.00}Ti_{0.01})_{\Sigma=2.01}[Al_{1.51}Si_{2.49}O_{10}](OH)_2$ or, ideally, $(Ba_{0.5}K_{0.5})Al_2(Al_{1.5}Si_{2.5})O_{10}(OH)_2$. This composition corresponds to the recently described mica, ganterite. Complete solid solutions between muscovite and ganterite were observed that range from 0.60% up to 18.12 wt% BaO. The electron-backscatter diffraction and Raman spectra of this phase are essentially indistinguishable from those of muscovite confirming that ganterite has a mica structure.

Keywords: Ganterite, mica, barium, Oreana, Nevada

INTRODUCTION

During our study of specimens of dumortierite from Oreana, Nevada, we found that the associated muscovite in one specimen contained unusually high concentrations of Ba. It is the purpose of this paper to characterize this mica. Previously, Ba-containing muscovite has been reported from numerous localities with BaO concentrations ranging up to 12 wt% (Dunn 1984; Dymek et al. 1983; Pan and Fleet 1991; Tracy 1991; Grapes 1993; Harlow 1995; Jiang et al. 1996), and the recently described mineral, ganterite (Graeser et al. 2003) with BaO ranging up to 17.15 wt%.

METHODS

The hand specimen, Caltech reference collection number CIT 1547, comes from the Lincoln Hill dumortierite deposit in the Humboldt Range located near Oreana, Pershing County, Nevada (Kerr and Jenny 1935). It is an approximately 7 cm hand specimen that is composed of small crystals of light-blue dumortierite associated with veins of cream-white barite and local areas of pale-lavender dumortierite. Polished thin sections of the specimen showed that the dumortierite and barite are intimately intermixed with a fine-grained micaceous mineral.

Back-scattered electron (BSE) images were obtained with a LEO 1550VP field emission SEM and a JEOL 733 electron microprobe. Regions enriched in heavy elements were subjected to detailed quantitative elemental microanalyses conducted with the JEOL 733 electron microprobe operated at 15 kV and 25 nA with a beam diameter of 1 µm. Standards for the analysis were albite (Na$K\alpha$), microcline (K$K\alpha$), anorthite (Si$K\alpha$, Al$K\alpha$, Ca$K\alpha$), rutile (Ti$K\alpha$), forsterite (Mg$K\alpha$), fayalite (Fe$K\alpha$), tephroite (Mn$K\alpha$), and benitoite (Ba$L\alpha$). Analyses were processed with the CITZAF correction procedure (Armstrong 1995). The electron microprobe data of the micas were carefully verified to assure that no contamination from barite was present.

Electron-backscatter diffraction (ESBD) analyses at a sub-micrometer scale were preformed using an HKL EBSD system on the LEO 1550VP, operated at 20 kV and 1 nA in a focused beam with a 70° tilted stage. The EBSD system was calibrated using a single crystal Si standard. Cell constants for the Ba mica were obtained by matching experimental EBSD pattern with modified 2M_1 muscovite structures.

* E-mail: chi@gps.caltech.edu

Raman spectroscopic microanalysis was carried out using a Renishaw M1000 micro-Raman spectrometer system on portions of the sample in thin section previously identified as Ba-rich through BSE images. Approximately 1 mw of 514.5 nm laser illumination (at the sample) focused with a 100× objective lens provided satisfactory spectra. The spot size was about 2 µm. Analyses were also conducted on regions identified with a low-Ba content. Peak positions were calibrated against an Si standard. A dual-wedge polarization scrambler was used in the laser beam for all spectra.

RESULTS

The electron microscope images show that the muscovite occurs in polycrystalline masses of mica that are a few hundred micrometers in size. Individual mica crystals are up to 100 micrometers in width. The mica is admixed with 50 to 400 µm dumortierite crystals, 10 to 400 µm blebs of barite, and trace amounts of 1 to 30 µm corundum crystals. Nano-sized barite crystals (down to 200 nm in thickness) also occur between muscovite layers. BSE imaging (Fig. 1) reveals that some regions of the muscovite contain areas of high concentrations of a heavy element.

Electron microprobe analyses of the micas (Table 1) show that the regions that contain barium have BaO concentrations ranging from 0.60 to 18.12 wt%. The mica with 18.12 wt% BaO shows an idealized mica composition corresponding to ganterite. The concentration of Na does not vary with Ba or K concentrations in the Oreana micas (Fig. 2). Aluminum dominates the octahedral sites where only traces of Ti and Fe are present. The ideal formula of Oreana ganterite, $(Ba_{0.5}K_{0.5})Al_2(Si_{2.5}Al_{1.5}O_{10})(OH)_2$, does not have the Na found in the ideal formula of the Berisal ganterite, $[Ba_{0.5}(Na+K)_{0.5}]Al_2(Si_{2.5}Al_{1.5}O_{10})(OH)_2$.

The EBSD patterns of the ganterite and the associated muscovite with very low Ba content are almost identical (Fig. 3). The patterns were obtained under the same SEM conditions. The improved sharpness of the ganterite pattern (Fig. 3a) is likely due to heavier Ba in the structure. The patterns were indexed to give

TABLE 1. Representative electron microprobe analyses of the Oreana mica

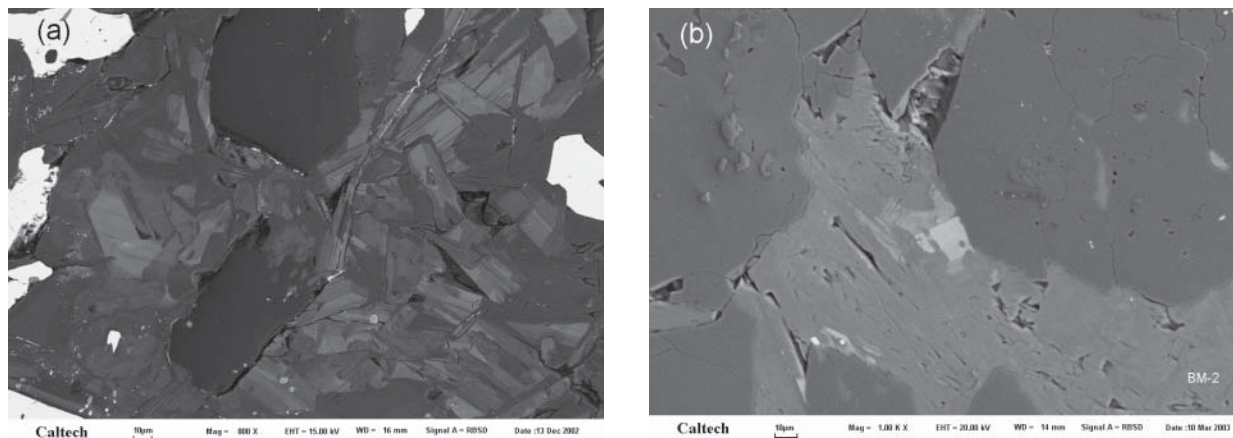|	Ganterite			Barian-muscovite			Muscovite
wt%							
Na₂O	0.36(1)	0.42(1)	0.37(1)	0.32(1)	0.30(1)	0.27(1)	0.31(1)
MgO	0.01(1)	0.00(1)	0.00(1)	0.00(1)	0.01(1)	0.07(1)	0.03(1)
Al₂O₃	40.20(8)	40.03(8)	38.95(8)	39.16(8)	38.19(8)	38.03(8)	38.42(8)
SiO₂	33.53(7)	36.02(7)	37.75(8)	40.48(8)	41.49(8)	44.64(9)	45.76(9)
K₂O	3.91(3)	4.91(3)	5.67(3)	7.00(4)	7.87(4)	9.36(5)	10.21(5)
CaO	0.04(1)	0.00(1)	0.00(1)	0.02(1)	0.01(1)	0.10(1)	0.01(1)
TiO₂	0.14(5)	0.19(3)	0.16(3)	0.04(5)	0.21(5)	0.03(4)	0.05(4)
MnO	0.04(1)	0.00(2)	0.00(2)	0.00(2)	0.00(2)	0.01(2)	0.01(2)
FeO	0.06(2)	0.05(2)	0.07(2)	0.09(2)	0.05(2)	0.13(2)	0.05(2)
BaO	18.12(51)	15.23(22)	12.85(22)	9.70(38)	7.37(33)	2.06(19)	0.60(13)
Total	96.42	96.85	95.82	96.82	95.50	94.69	95.44
Formula based on 11 O atoms							
Ba	0.526	0.430	0.361	0.263	0.200	0.054	0.015
K	0.370	0.452	0.518	0.618	0.694	0.801	0.860
Na	0.052	0.058	0.051	0.043	0.040	0.035	0.040
Ca	0.003	0.000	0.000	0.001	0.001	0.007	0.001
Al(VI)	1.996	1.996	1.988	1.996	1.981	2.003	2.009
Mg	0.001	0.000	0.000	0.000	0.001	0.007	0.003
Ti	0.008	0.010	0.009	0.002	0.011	0.001	0.002
Mn	0.002	0.000	0.000	0.000	0.000	0.000	0.001
Fe	0.004	0.003	0.004	0.005	0.003	0.007	0.003
Si	2.485	2.596	2.702	2.802	2.869	2.996	3.020
Al(IV)	1.515	1.404	1.298	1.198	1.131	1.004	0.980
∑ cations	6.963	6.949	6.931	6.929	6.931	6.918	6.933

FIGURE 1. (**a**) A typical back-scattered electron image of a thin section of the Oreana dumortierite. Pure white areas are barite, solid dark areas are dumortierite, and the patterned area consists of mica crystals. The lighter color corresponds to greater heavy element (Ba) contents. Scale bar = 0.01 mm. (**b**) A back-scattered electron image of a thin section of the Oreana dumortierite centered on mica. The brightest zone near the center of the image is a Ba-rich zone that was the focus of the analyses of this paper. Scale bar = 0.01 mm.

a best fit based on $2M_1$ muscovite structure (Fig. 3c), showing a = 0.519 nm, b = 0.900 nm, c = 2.004 nm, β = 95.7°, all of which are consistent with ganterite (Graeser et al. 2003).

Electron microprobe analyses showed that F is absent from the mica. The Raman spectra (Fig. 4a) gave clear evidence for OH in the Ba-rich mica with a band at about 3627 cm⁻¹ that had a higher-energy shoulder at about 3655 cm⁻¹. An OH band with similar intensity was also observed in the Raman spectrum of the nearby muscovite.

Raman spectra (Fig. 4b) reveal that the most Ba-rich mica has the same features as the associated low-Ba muscovite and is effectively undistinguishable from muscovite in this wavenumber range. Both of these patterns correspond to standard muscovite

patterns in commercial and in-house databases of Raman spectra. The Berisal ganterite has a different Raman spectrum (Fig. 5). Although it has the same features found in the spectrum of Figure 4, it displays other bands in addition that are not found in the spectrum of the Oreana mica. These include a series of bands in the 920 to 1020 cm⁻¹ region and prominent bands near 440 and 605 cm⁻¹.

DISCUSSION

It is evident that ganterite is a dioctahedral layer silicate whose ideal composition is located halfway between the true micas and the brittle micas. The chemical formula suggests that this phase could be an ordered 1:1 interstratification of muscovite
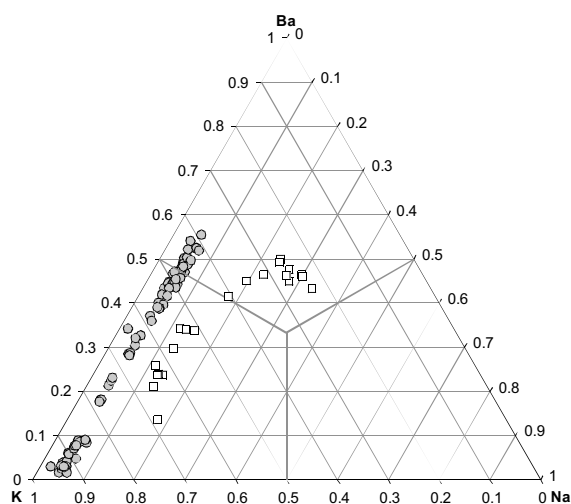
FIGURE 2. Ternary plot of the interlayer cations in barian micas. Circles: Oreana micas (this study); squares: Berisal micas (Graeser et al. 2003; Hetherington et al. 2003).
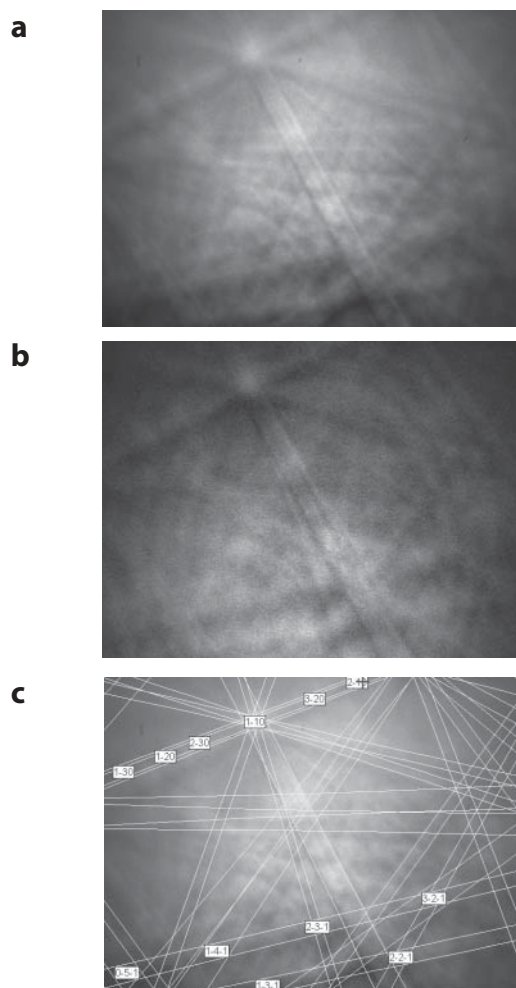

FIGURE 3. EBSD patterns of (**a**) the Ba mica; (**b**) the adjacent muscovite; (**c**) an indexed pattern of **a**.
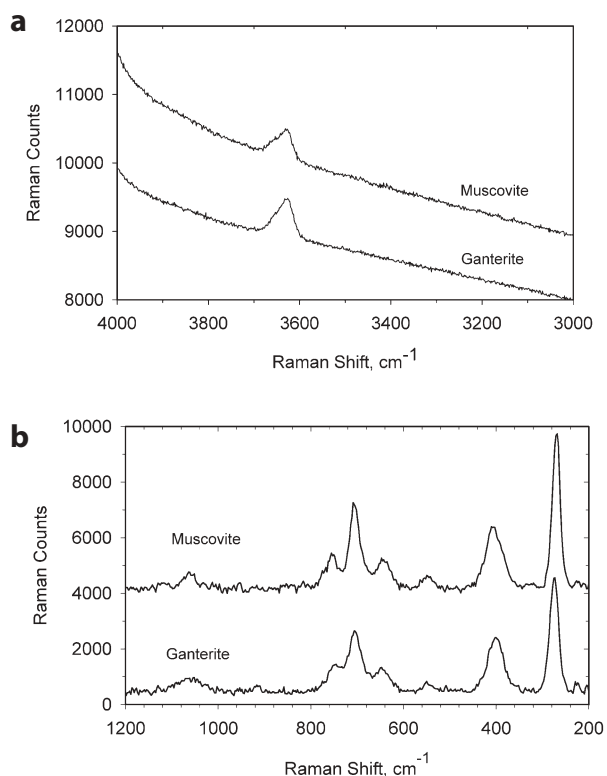

FIGURE 4. Raman spectra of the most Ba-rich mica (ganterite) and the adjacent low-Ba muscovite from Oreana, Nevada. (**a**) The OH region and (**b**) the lower wavenumber region.

and Ba brittle mica. Alternatively, because the ionic radii of K^+ (164 pm) and Ba^{2+} (161 pm) are very close in 12-coordination (Shannon 1976), the K and Ba could be statistically distributed in the interlayers with corresponding substitutions in the tetrahedral layers. Further high-resolution TEM and selected-area electron diffraction examinations of specimens are required to establish the structural nature of this Ba mica.

The Oreana ganterite formed by hydrothermal alteration, along with muscovite, dumortierite, and barite (Kerr and Jenny 1935). It is different morphologically, chemically, and maybe even structurally, from the Berisal ganterite that formed by Alpine metamorphism. The Oreana mica is much smaller in size and its composition reaches almost a pure 50/50 mix of the hypothetical brittle mica, $BaAl_2(Si_2Al_2)O_{10}(OH)_2$, and muscovite, $KAl_2(Si_3Al)O_{10}(OH)_2$. In contrast, the Berisal ganterite crystals are relatively much larger at a sub-millimeter to millimeter scale with high Na in the interlayer cation sites (Na/K atomic ratio ≈ 1) and significant Mg, Fe, and Ti substitutions for Al in the octahedral sites (Graeser et al. 2003). Brigatti et al. (1998) reported that the replacement of ^{VI}Al by Mg, Fe, and Ti in muscovite-$2M_1$ expands the octahedral sheet and gives rise to a more hexagonal tetrahedral ring and low corrugation of the basal O plane. Structure refinements of barian muscovites from the Berisal Complex (Armbruster et al. 2002) showed that the Berisal barian muscovite with Ba contents between 0.05 and 0.35 pfu has a smaller cell volume than that of ideal muscovite because of its paragonite content (Na concentration between 0.13 and 0.2 pfu). It is obvious
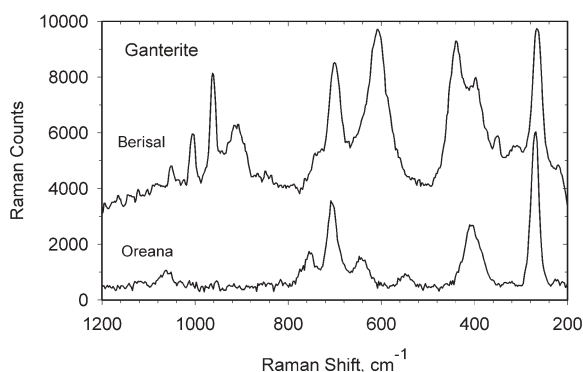
FIGURE 5. Raman spectra of the Oreana and Berisal ganterites. The intensity of the Berisal spectrum (digitized from Graeser et al. 2003) was scaled to be similar to the Oreana pattern (this study).

that the Berisal ganterite with a phengitic substitution (near 10% Al octahedral sites filled with Mg, Fe, and Ti) and a significant paragonite component (near 25% interlayer sites occupied with Na) (Graeser et al. 2003) might have a slightly different structure, whereas the Oreana ganterite displays a structure almost identical to pure muscovite. These structural and compositional differences might be a reason that the Berisal ganterite exhibits a different Raman spectrum (Fig. 5).

Our compositional data show that Ba occupies more than 50% of the interlayer cation sites, which suggests that the Oreana ganterite may be more a brittle mica than a true mica. This finding also marks the Oreana ganterite as the most Ba-enriched dioctahedral mica reported to date. The results of Graeser et al. (2003) showed that the Berisal ganterite is chemically a true mica because Ba does not occupy more than 50% of the interlayer cation sites in the empirical formula.

Graeser et al. (2003) concluded that the increasing concentrations of Ba and Al in the mica are also correlated with increases in Na. Thus, they concluded that ganterite does not participate in a simple binary solid-solution with muscovite, but rather, it was involved with a more complicated ternary solid-solution that includes paragonite. Although our data do not rule out the ternary solid-solution that was evident in the Berisal ganterite, the low but constant Na contents of our data do suggest that a purely binary K-Ba solid-solution exists.

Barium muscovite is widely reported to be associated with metasomatic processes (Harlow 1995). Our results raise the possibility that ganterite may be present in those localities where Ba-rich muscovite has been found. Because ganterite may exist at micrometer to nanometer scales, as is the case for the Oreana locality, this phase can be easily missed during SEM and electron microprobe studies. The presence of barite along with fine-grained mica might be a key indicator of ganterite formation.

REFERENCES CITED

Armbruster, T., Berlepsch, P., Gnos, E., and Hetherington, C.J. (2002) Crystal chemistry and structure refinements of barian muscovites from the Berisal Complex, Simplon region. Schweizerische Mineralogische und Petrographische Mitteilungen, 82, 537–547.

Armstrong, J.T. (1995) CITZAF: a package of correction programs for the quantitative electron microbeam X-ray analysis of thick polished materials, thin films, and particles. Microbeam Analysis, 4, 177–200.

Brigatti, M.F., Frigieri, P., and Poppi, L. (1998) Crystal chemistry of Mg-, Fe-bearing muscovite-$2M_1$. American Mineralogist, 83, 775–785.

Dunn, P.J. (1984) Barian muscovite from Franklin, New Jersey. Mineralogical Magazine, 48, 562–563.

Dymek, R.F., Boak, J.L., and Kerr, M.T. (1983) Green micas in the Archean Isua and Malene supracrustal rocks, southern West Greenland, and the occurrence of a barian-chromian muscovite. Rapport—Grønlands Geologiske Undersøgelse, 112, 71–82.

Graeser, S., Hetherington, C.J., and Giere, R. (2003) Ganterite, a new barium-dominant analogue of muscovite from the Berisal Complex, Simplon Region, Switzerland. Canadian Mineralogist, 41, 1271–1280.

Grapes, R.H. (1993) Barian mica and distribution of barium in metacherts and quartzofeldspathic schists, Southern Alps, New Zealand. Mineralogical Magazine, 57, 265–272.

Harlow, G.E. (1995) Crytal chemistry of barian enrichment in micas from metasomatized inclusions in serpentinite, Motagua Fault Zone, Guatemala. European Journal of Mineralogy, 7, 775–789.

Hetherington, C.J., Giere, R., and Graeser, S. (2003) Composition of barium-rich white micas from the Berisal Complex, Simplon Region, Switzerland. Canadian Mineralogist, 41, 1281–1291.

Jiang, S.-Y., Palmer, M.R., Li, Y.-H., and Xue, C.-J. (1996) Ba-rich micas from the Yindongzi-Daxigou Pb-Zn-Ag and Fe deposits, Qinling, northwestern China. Mineralogical Magazine, 60, 433–445.

Kerr, P.K. and Jenny, P. (1935) The dumortierite-andalusite mineralization at Oreana, Nevada. Economic Geology and the Bulletin of the Society of Economic Geologists, 30, 287–300.

Pan, Y. and Fleet, M.E. (1991) Barian feldspar and barian-chromium muscovite from the Hemlo area, Ontario. Canadian Mineralogists, 29, 481–498.

Shannon, R.D. (1976) Revised effective ionic radii and systematic studies of interatomic distances in halides and chalcogenides. Acta Crystallographica, A32, 751–767.

Tracy, R.J. (1991) Ba-rich micas from the Franklin Marble, Lime Crest and Sterling Hill, New Jersey. American Mineralogist, 76, 1683–1693.